F05

Proceedings of the 5th International Conference on Inverse Problems in Engineering: Theory and Practice, Cambridge, UK, 11-15th July 2005

ESTIMATION OF THE THERMAL RESISTANCE DISTRIBUTION OF DIE-ATTACH MATERIALS IN MICROELECTRONICS

V. FEUILLET[1], Y. JARNY[1] and Y. SCUDELLER[2]
[1] *Laboratoire de Thermocinétique, UMR-CNRS 6607*
[2] *Laboratoire de Génie des Matériaux et Procédés Associés*
Ecole Polytechnique de l'Université de Nantes
La Chantrerie, rue Christian Pauc, BP 50609, 44306 Nantes, France
e-mail: vincent.feuillet@univ-nantes.fr

Abstract – In the present study a three-dimensional steady-state inverse heat conduction problem is solved using the conjugate gradient method to estimate the thermal resistance distribution of die-attach materials used in microelectronics. The thermal performance of such interface materials is of critical concern for engineers due to the power increase of microelectronics systems. The spatial distribution of the thermal resistance is obtained from temperature measurements at the top of the semiconductor device. Numerical experiments are performed in two different measurement situations (electrothermal method and infrared thermography). Results show the influence of the heat source configuration and of the measurement errors on the numerical solution of the inverse problem.

1. INTRODUCTION

Interface materials (adhesives, soft and hard solders…) are used as die-attach layers of power integrated circuits. Thermal properties of these interfaces play an essential role on the temperature of semiconductor junctions and have consequently a strong impact on reliability and cooling performances. The presence of defects (voids, dislocations) introduces thermal resistances that lead to temperature drops at the interfaces. So interface thermal phenomena are at the origin of a large part of the overheating of the device and of the presence of hot spots.

Thermal resistance of die-attach materials is usually represented by one parameter by assuming uniform distribution at the interface. This single parameter has been estimated in numerous thermal characterizations of electronics systems. For instance, Gatto [3] measured the thermal resistance of adhesives interfaces used in hybrid power components. Maranzana [5] characterized SiO_2 layers found in IGBT (Insulated Gate Bipolar Transistor) modules. Prasher *et al.* [7] investigated the thermal contact resistance of Phase Change Materials in an actual CPU (Central Processing Unit) heat sink installation. Raiszadeh and Derian [8] studied the thermal resistance of a new interface technology constituted by a corrugated copper substrate with thermal grease. But in practice, structural interface defects are not uniformly distributed and their location influences the temperature of the semiconductor device. This influence could become crucial in the case of harsh thermomechanical fatigue that tends to unstick the corners of adhesives layers or leads to the development of cracks in solders. The estimation of a non-uniform thermal resistance in multi-dimensional problem is very limited in the literature. Bendada *et al.* [2] reconstituted a profile of interface thermal resistance but it concerns a two-dimensional problem.

The objective of this paper is to evaluate the interface thermal resistance distribution of a die-attach material thanks to a non-destructive experiment. This involves the development of a suitable inverse methodology. The direct problem is based on an original thermal model that solves the 3-D heat conduction equation in steady state conditions through a two-block electronic structure. It enables us to take into account a spatial distribution of the interface thermal resistance. The inverse problem consists in minimizing a functional that links the estimated and the measured temperatures taken at the top of the structure. An iterative process based on the conjugate gradient method is used for the minimization of this functional. Two different approaches are considered for the simulation of the temperature measurements: the average temperatures of the heat sources are available by simulating an electrothermal method or a quite detailed grid of temperature measurements is known thanks to infrared thermography. The influence of the measurement errors are investigated and several results are presented concerning the accuracy and the convergence rate of the inverse computation.

2. DIRECT PROBLEM

2.1 Modeling

Let us consider the problem of a semiconductor device (element 1) attached on a heat spreader (element 2) as shown in Figure 1:

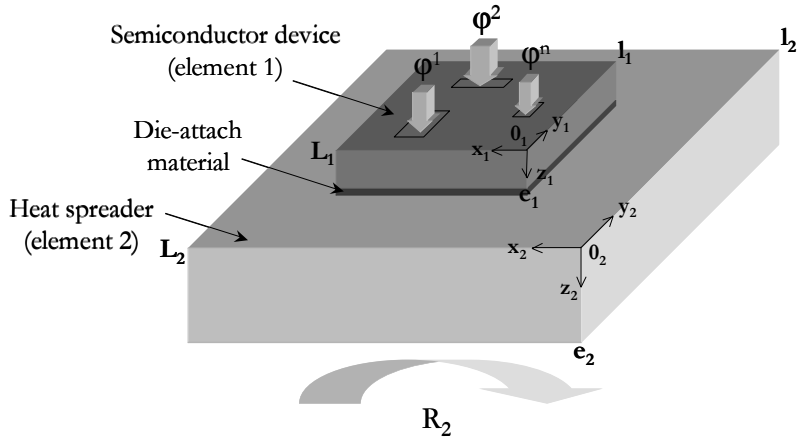

Figure 1. Semiconductor device attached on a heat spreader.

The upper face of the semiconductor device is submitted to a set of n heat sources due to the heat dissipation of elementary electronic components (transistors, diodes, thyristors…). The lower face of the heat spreader is submitted to a thermal resistance R_2 that could be non-uniform. This coefficient is determined by the quality of the contact between the heat spreader and the heat sink of the system. The interface between the two elements is typically composed of a die-attach material suitable for the cooling of microelectronics structures: adhesive, soft or hard solder, thermal grease, Phase Change Material (PCM), composite… This interface is much thinner than other layers and is usually represented in simulations by an interface thermal resistance. This approach consists in considering the thickness of the interface as zero and replacing it by a temperature discontinuity. We assume in this study that this interface thermal resistance is not uniformly distributed.

The technique used to solve the direct problem in steady state conditions is to consider each element (semiconductor and heat spreader) as a piecewise homogeneous and to solve them separately. The mathematical formulation of each stationary heat conduction problem (i=1 or 2) is given as follows:

$$\frac{\partial^2 T_i}{\partial x_i^2} + \frac{\partial^2 T_i}{\partial y_i^2} + \frac{\partial^2 T_i}{\partial z_i^2} = 0 \text{ in element } I \tag{1}$$

$$\frac{\partial T_i}{\partial x_i} = 0 \text{ at } x_i = 0 \text{ and } x_i = L_i \tag{2}$$

$$\frac{\partial T_i}{\partial y_i} = 0 \text{ at } y_i = 0 \text{ and } y_i = l_i \tag{3}$$

$$-\lambda_i \frac{\partial T_i}{\partial z_i} = \varphi_{up_i}(x_i, y_i) \text{ at } z_i = 0 \tag{4}$$

$$-\lambda_i \frac{\partial T_i}{\partial z_i} = \frac{T_i - T_\infty}{R_i(x_i, y_i)} \text{ at } z_i = e_i \tag{5}$$

where T_i is the temperature distribution in the element i, λ_i is its thermal conductivity, φ_{up_i} is the heat flux density distribution prescribed on the upper face of the element i, T_∞ is the uniform temperature reference of the heat sink and R_i is the thermal resistance distribution established between the lower face of the element i and the heat sink. We should note that eqn.(5) must be seen as a boundary condition of the third kind where $R_i(x_i,y_i)$ is the inverse of a non-uniform heat transfer coefficient. R_2 is fixed by the contact of the heat spreader with the heat sink and is supposed to be known whereas R_1 is given by:

$$R_1(x_1, y_1) = R_{int}(x_1, y_1) + \frac{T_{up_2}(x_2^{int}, y_2^{int}) - T_\infty}{\varphi_{up_2}(x_2^{int}, y_2^{int})} \tag{6}$$

where T_{up_2} is the temperature distribution on the upper face of the element 2 and R_{int} is the interface thermal resistance distribution of the die-attach material that is known in the direct problem. The superscript ‘‘*int*‘‘ means that it concerns the points at the interface. The principle of the computation method is to develop an iterative process that determines the effective thermal resistance distribution $R_1(x_1,y_1)$.

2.2 Solution using the thermal quadrupole method

The two separated problems are solved by using the thermal quadrupole method based on integral transforms, [6]. This technique allows us to link the temperature-heat flux density spectrum vectors at the upper face of the element to the corresponding vectors at the heat sink thanks to transfer matrices:

$$\begin{bmatrix} \widetilde{\theta}(up) \\ \widetilde{\Phi}(up) \end{bmatrix} = \begin{bmatrix} A & B \\ C & D \end{bmatrix} \begin{bmatrix} I & \widetilde{R} \\ 0 & I \end{bmatrix} \begin{bmatrix} \widetilde{\theta}(\infty) \\ \widetilde{\Phi}(\infty) \end{bmatrix} \tag{7}$$

where

$$\widetilde{\theta} = [\widetilde{\theta}_{0,0} \;\leftrightarrow\; \widetilde{\theta}_{N,0} \;\cdots\; \widetilde{\theta}_{0,m} \;\leftrightarrow\; \widetilde{\theta}_{N,m} \;\cdots\; \widetilde{\theta}_{0,M} \;\leftrightarrow\; \widetilde{\theta}_{N,M}]^t \tag{8}$$

and

$$\widetilde{\Phi} = [\widetilde{\Phi}_{0,0} \;\leftrightarrow\; \widetilde{\Phi}_{N,0} \;\cdots\; \widetilde{\Phi}_{0,m} \;\leftrightarrow\; \widetilde{\Phi}_{N,m} \;\cdots\; \widetilde{\Phi}_{0,M} \;\leftrightarrow\; \widetilde{\Phi}_{N,M}]^t \tag{9}$$

with $\widetilde{\theta}_{n,m}$ and $\widetilde{\Phi}_{n,m}$ the double Fourier cosine transforms of the temperature T and the heat flux density φ:

$$\widetilde{\theta}_{n,m}(z) = \int_{x=0}^{L}\int_{y=0}^{l} T(x,y,z)\cos(\alpha_n x)\cos(\beta_m y)dxdy \qquad \widetilde{\Phi}_{n,m}(z) = \int_{x=0}^{L}\int_{y=0}^{l} (-\lambda\frac{\partial T}{\partial z})\cos(\alpha_n x)\cos(\beta_m y)dxdy \tag{10}$$

Here n and m are respectively the nth and mth harmonics in the x and y directions. N and M are the corresponding truncation orders. α_n and β_m are the eigenvalues in the x and y directions:

$$\alpha_n = \frac{n\pi}{L} \qquad \beta_m = \frac{m\pi}{l} \tag{11}$$

A, B, C and D are square diagonal matrices. A is given by:

$$A = diag(A_{0,0} \;\leftrightarrow\; A_{N,0} \;\cdots\; A_{0,m} \;\leftrightarrow\; A_{N,m} \;\cdots\; A_{0,M} \;\leftrightarrow\; A_{N,M}) \tag{12}$$

with

$$A_{n,m} = \cos(\gamma_{n,m}e) \tag{13}$$

B, C and D are calculated the same way with:

$$B_{n,m} = \frac{\sinh(\gamma_{n,m}e)}{\lambda\gamma_{n,m}} \qquad C_{n,m} = \lambda\gamma_{n,m}\sinh(\gamma_{n,m}e) \qquad D_{n,m} = \cosh(\gamma_{n,m}e) \tag{14}$$

$\gamma_{n,m}$ depends on the eigenvalues α_n and β_m and is given by:

$$\gamma_{n,m}^2 = \alpha_n^2 + \beta_m^2 \tag{15}$$

I is the identity matrix whose size is the total of harmonics kept ((N+1)(M+1)×(N+1)(M+1)). $\widetilde{R}$ is a convolution matrix with the same size that depends on the thermal resistance distribution $R(x,y)$. The calculation of the analytical coefficients of $\widetilde{R}$ requires a discretization of the lower face of the element. This face is typically discretized into a regular grid of 30×30 points to obtain accurate results. The details of this calculation are given in [6].

This formulation leads to solve a two-equation system with two unknowns: the spectrum vector of the temperature at the upper face of the element $\widetilde{\theta}(up)$ and the spectrum vector of the heat flux density at the heat sink $\widetilde{\Phi}(\infty)$. Indeed, the heat flux density distribution at the upper face of the element is known (φ_{up}) and the same for the temperature of the heat sink (T_∞). Note that this solving requires to invert a (N+1)(M+1)×(N+1)(M+1) matrix. Once these two unknown spectra have been computed, we return to the space domain by using the following inverse expression (for the temperature for example):

$$T(x,y,z) = \sum_{n=0}^{N}\sum_{m=0}^{M}\frac{\widetilde{\theta}_{n,m}(z)}{N_{n,m}}\cos(\alpha_n x)\cos(\beta_m y) \tag{16}$$

where $N_{n,m}$ is the norm of the scalar product:

$$N_{n,m} = \int_{x=0}^{L}\int_{y=0}^{l}\cos^2(\alpha_n x)\cos^2(\beta_m y)dxdy \tag{17}$$

2.3 Iterative algorithm for solving the direct problem

The previous solution has to be integrated into an original iterative algorithm. The process is initialized by setting an initial distribution $R_1^0(x_1, y_1)$. Thus we obtain the heat flux density distribution at the lower face of the element 1 by solving the heat conduction problem for i=1. This distribution is prescribed into the upper face

of the element 2 ($\varphi^0_{up_2}(x_2, y_2)$) because of the continuity of the heat flux density through the interface. Then the heat conduction problem in the element 2 can be solved and leads to the temperature distribution $T^0_{up_2}(x_2, y_2)$ to compute a second distribution $R^1_1(x_1, y_1)$ given by:

$$R^1_1(x_1, y_1) = R_{int}(x_1, y_1) + \frac{T^0_{up2}(x_2^{int}, y_2^{int}) - T_\infty}{\varphi^0_{up_2}(x_2^{int}, y_2^{int})} \tag{18}$$

This calculation loop is repeated until the convergence of the distribution $R^j_1(x_1, y_1)$. The detailed principle of this iterative process is given on Figure 2:

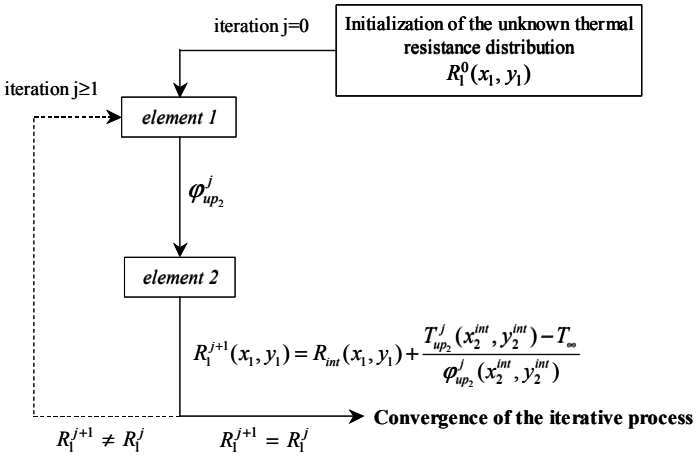

Figure 2. Principle of the iterative process for solving the 3-D heat conduction direct problem.

2.4 Validation of the direct problem

The thermal model is validated by simulating a RF (Radio Frequency) Power Component and comparing the results with those given by the Finite-Element code Femlab. We study the structure described in Table 1 and Figure 3. The contact between the element 2 and the heat sink is assumed to be perfect (R_2=1.10^{-10} K.m^2.W^{-1}) and the temperature of the heat sink T_∞ is set equal to 0°C. The die-attach material is supposed to be an adhesive with a lack of contact on one corner, the corresponding interface thermal resistance distribution is simulated by a spatial sinusoidal function (see Figure 4).

	λ (W.m^{-1}.K^{-1})	L (mm)	l (mm)	e (mm)
Element 1 (AsGa)	44	3.08	1.26	0.1
Element 2 (CuW)	150	4.71	2.5	0.5

Table 1. Thermal properties and dimensions of the structure for the validation of the direct problem.

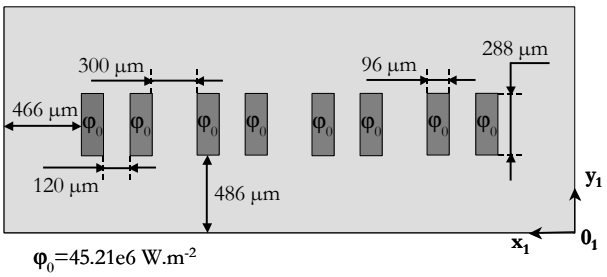

Figure 3. Heat source configuration on the upper face of element 1 for the validation of the direct problem.

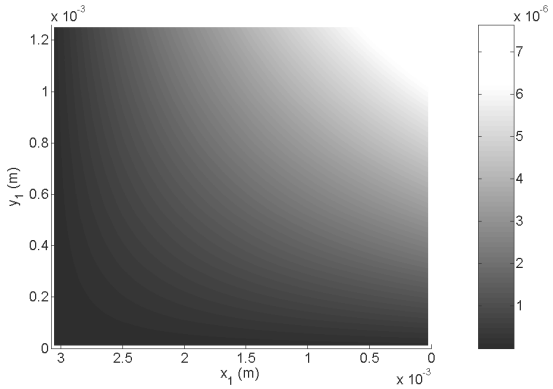

Figure 4. Interface thermal resistance distribution (K.m^2.W^{-1}): R_{int}=2sin((L$_1$-x$_1$)y$_1$) - validation of the direct problem.

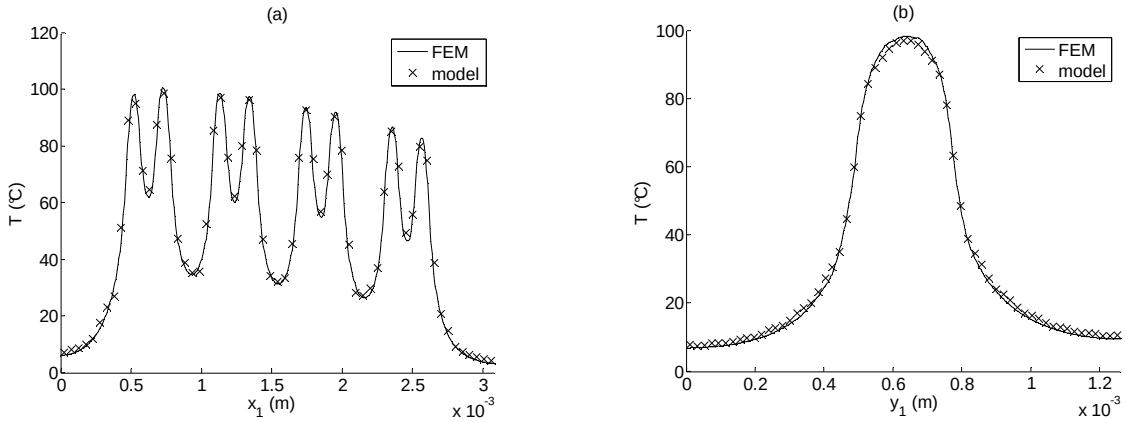

Figure 5. Validation of the direct problem - temperature profiles on the upper face of element 1: (a) for y_1=0.63 mm, (b) for x_1=1.13 mm.

As we can see on Figure 5, the results of the model are in very good accordance with the Finite Element Method. The differences between the two methods remain lower than 3°C. We clearly observe on these temperature profiles the influence of the non-uniformity of the interface thermal resistance.

We should add that this model has been generalized to n-layer electronic structures and has given quite satisfactory results in terms of accuracy and time computation costs by comparing with the Finite Element Method. Note that this model does not require to mesh the entire structure, which represents an important advantage with such 3-D geometries (small thickness compared to the other dimensions of the element, very different scales between elements).

3. INVERSE PROBLEM

3.1 Formulation of the three-dimensional steady-state inverse heat conduction problem

The interface thermal resistance distribution $R_{int}(x_1, y_1)$ is regarded as the unknown of the inverse problem, the other variables of the previous direct problem being known. We consider available some temperature measurements on the upper face of the element 1 to estimate $R_{int}(x_1, y_1)$.

We suppose that the heat sources are constituted by some electrolytic deposits heated by an electrical current that provides the power supply. Two different measurement methods are simulated in steady state conditions. First, we study an electrothermal method that gives the average temperature of the heat sources thanks to a conversion from the electrical resistance of the electrolytic deposits to their average temperature. Then we examine the case of the infrared thermography that provides the temperature at some grid locations linked to the resolution of the infrared camera.

The interface is discretized in the direct problem into a regular grid in which we assume that the interface thermal resistance is constant on a given number of zones. These zones are defined by dividing the interface into *nb* zones of equal areas:

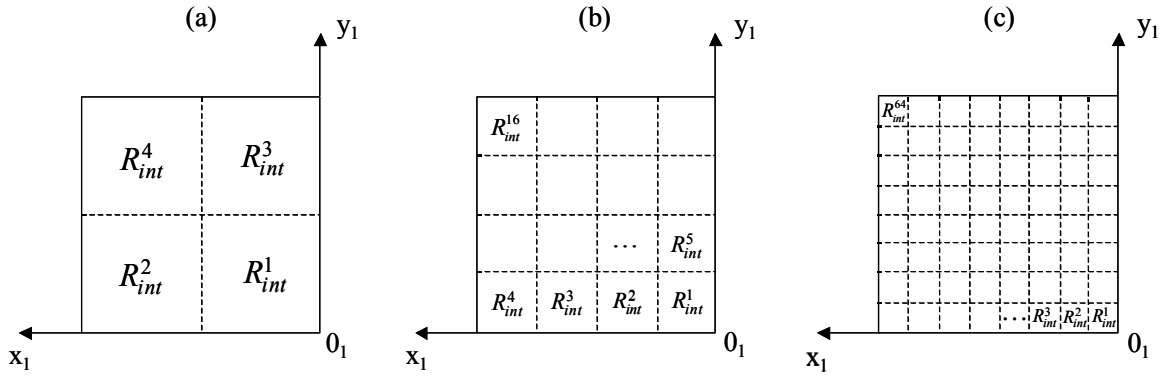

Figure 6. Partitions of the interface into nb zones of constant thermal resistance: (a) 4-zone partition, (b) 16-zone partition, (c) 64-zone partition.

So the objective of the inverse problem is to search a *nb*-component vector, with *nb* the number of zones of constant interface thermal resistance:

$$R_{int} = [R_{int}^1 \;;\; R_{int}^2 \;;\; \cdots \;;\; R_{int}^i \;;\; \cdots \;;\; R_{int}^{nb}]^t = [R_{int}^i]_{i=1}^{i=nb} \tag{19}$$

The inverse analysis aims at determining the unknown vector R_{int} from the temperature measurements denoted by Y_i, i=1 to I, where I represents the number of heat sources in the case of the electrothermal method or the number of grid locations of the camera in the case of the infrared thermography. This problem is formulated in the least-square sense and consists in finding the optimal solution that minimizes the functional:

$$J(\hat{R}_{int}) = \frac{1}{2}\left\| Y - \hat{\eta}(\hat{R}_{int}) \right\|^2 = \frac{1}{2}\sum_{i=1}^{I}\left(Y_i - \hat{\eta}_i(\hat{R}_{int})\right)^2 \tag{20}$$

where $\hat{\eta}(\hat{R}_{int})$ are the estimated temperatures determined from the solution of the direct problem by using an estimated vector $\hat{R}_{int}$. The superscript ‘‘^‘‘ denotes the estimated quantities.

3.2 The conjugate gradient method for minimization

An iterative process based on the conjugate gradient method is used for the estimation of R_{int} to minimize the functional J, [4]. At each iteration k, the previous estimation $\hat{R}_{int}^k$ is corrected according to:

$$\hat{R}_{int}^{k+1} = \hat{R}_{int}^k + \rho^k w^k \tag{21}$$

in order to obtain:

$$J\left(\hat{R}_{int}^{k+1}\right) < J\left(\hat{R}_{int}^k\right) \tag{22}$$

where ρ^k is the search step size and w^k is the direction of descent.

The vector w^k is determined with the conjugate gradient equations:

$$w^k = -\nabla J^k + \gamma^k w^{k-1} \tag{23}$$

$$\gamma^0 = 0 \tag{24}$$

$$\gamma^k = \frac{\left\|\nabla J^k\right\|^2}{\left\|\nabla J^{k-1}\right\|^2} = \frac{(\nabla J^k)^t(\nabla J^k)}{(\nabla J^{k-1})^t(\nabla J^{k-1})} \tag{25}$$

with ∇J the gradient vector of the functional J. The components of ∇J are given by:

$$\nabla J_i = \frac{\partial J}{\partial \hat{R}_{int}^i}, \quad i = 1, 2, ..., nb \tag{26}$$

The gradient vector is calculated by solving the sensitivity equations.

The positive scalar ρ^k is the minimum of the one variable function:

$$\Phi(r) = J(\hat{R}_{int}^{k+1}) = J(\hat{R}_{int}^k + r w^k) \tag{27}$$

A linearization of this equation leads to the expression of ρ^k as follows:

$$\rho^k = \frac{(\nabla J^k)^t \nabla J^k}{(\nabla \hat{\eta}^k \nabla J^k)^t \nabla \hat{\eta}^k \nabla J^k} = \frac{(\nabla J^k)^t \nabla J^k}{(X^k \nabla J^k)^t X^k \nabla J^k} \tag{28}$$

where $\nabla\hat{\eta}$ is the gradient vector of the estimated temperatures and is defined as the sensitivity matrix denoted by X. This matrix is obtained by solving the sensitivity problem.

3.3 The sensitivity problem

The gradient vector ∇J is obtained from eqn.(20) in the following manner:

$$\nabla J = -\nabla \hat{\eta}^t \left(Y - \hat{\eta}\right) = -X^t \left(Y - \hat{\eta}\right) \tag{29}$$

Let ΔR be a variation of the interface thermal resistance. The components of X are defined by:

$$X_i = \lim_{\varepsilon \to 0} \frac{\hat{\eta}\left(\left[\hat{R}_{int}^j + \delta_i^j \varepsilon \Delta R\right]_{j=1}^{j=nb}\right) - \hat{\eta}\left(\left[\hat{R}_{int}^j\right]_{j=1}^{j=nb}\right)}{\varepsilon \Delta R} \text{ with } \delta_i^j = \begin{cases} 1 \text{ if } i=j \\ 0 \text{ if } i \neq j \end{cases} \text{ for } i=1, 2, \ldots, nb \tag{30}$$

In practice, the value of $\varepsilon\Delta R$ is chosen as:

$$\varepsilon \Delta R < 0.1\% \times \sqrt{\sum_{i=1}^{nb} (\hat{R}_{int}^i)^2} \tag{31}$$

Finally the sensitivity problem is solved by computing *nb* times the eqn.(30) and deducing the different components of the gradient vector ∇J with eqn.(29).

3.4 Computational procedure

The computational procedure for the solution of this inverse problem may be summarized as follows:

- $k \leftarrow 0$: choose an initial distribution $\hat{R}_{int}^{0}(x_1, y_1)$.
- Repeat:

Step 1. Solve the direct problem given by eqns (1) to (6) with $R_{int}(x_1, y_1) = \hat{R}_{int}^{k}(x_1, y_1)$ to compute $\hat{\eta}\left(\hat{R}_{\text{int}}^{k}\right)$.

Step 2. Compute the functional $J\left(\hat{R}_{\text{int}}^{k}\right)$ from eqn.(20) and examine the stopping criterion: $J\left(\hat{R}_{\text{int}}^{k}\right) < \varepsilon$, with ε a small-specified number. Stop the iterative process if satisfied, continue if not.

Step 3. Solve the sensitivity problem to compute the sensitivity matrix X given by eqn.(30) and the gradient vector $\nabla J\left(\hat{R}_{\text{int}}^{k}\right)$ given by eqn.(29).

Step 4. Compute the direction of descent w^k from eqns (23) to (25).

Step 5. Compute the step size ρ^k given by eqn.(28).

Step 6. Compute the new estimation $\hat{R}_{int}^{k+1}(x_1, y_1)$ from eqn.(21).

Step 7. $k \leftarrow k+1$: return to *Step 1*.

4. RESULTS AND DISCUSSION

In this section, we study the validity of our inverse method in predicting the interface thermal resistance distribution of a die-attach material from temperature measurements at the top of the structure. In all the test cases, we consider the attachment of a RF semiconductor in AsGa (λ_1=44 W.m^{-1}.K^{-1}) on a heat spreader in CuW (λ_2=150 W.m^{-1}.K^{-1}), as shown in Figure 7. We suppose that the heat spreader is perfectly cooled on its lower face (R_2=1.10^{-20} K.m^2.W^{-1}).

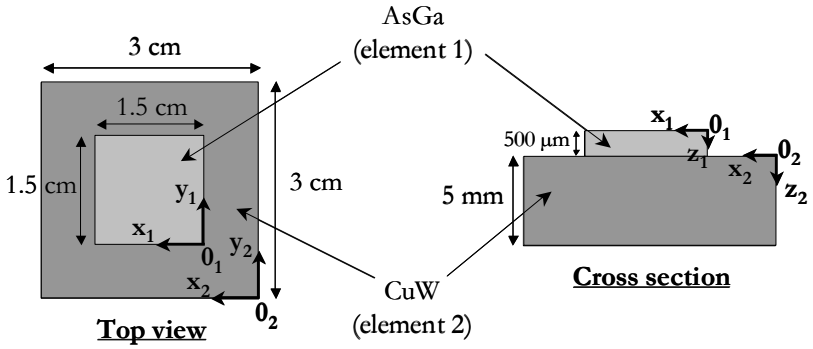

Figure 7. RF structure studied in the numerical experiments.

An adhesive constitutes the interface and its thermal resistance is supposed to vary with the position according to the following function:

$$f(x_1, y_1) = 5.10^{-2} \sin(x_1 \times y_1) \tag{32}$$

The exact distribution of the interface thermal resistance depends on the number of zones of constant interface thermal resistance, that is to say the number of components of the vector R_{int}. Three cases will be investigated (see Figure 8): a 4-component vector, a 16-component vector and a 64-component vector. The objective now is to choose a heat source configuration on the upper face of the element 1 suitable for the estimation of each component of the vector R_{int}.

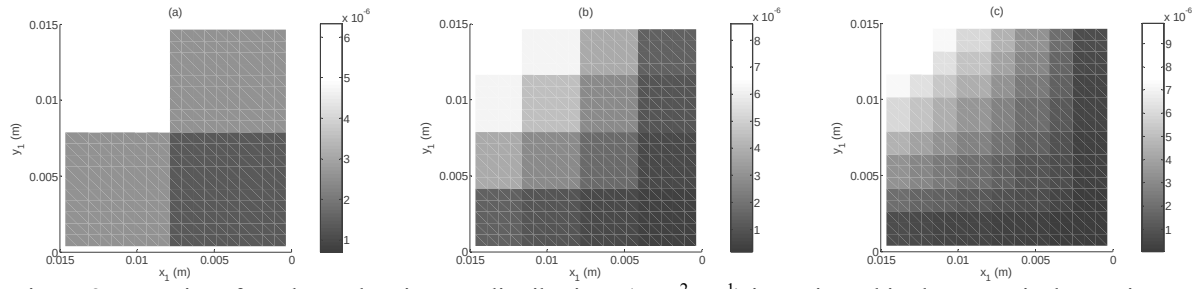

Figure 8. Exact interface thermal resistance distributions (K.m^2.W^{-1}) investigated in the numerical experiments: (a) 4-component vector, (b) 16-component vector, (c) 64-component vector.

Moreover, the temperature measurements are simulated by taking into account random measurement errors. The simulated experimental data can be expressed as:

$$Y_i = Y_i^{exact} + \sigma\omega_i \quad \text{for } i=1 \text{ to } I \tag{33}$$

where Y_i^{exact} is the solution of the direct problem with the exact distribution of the interface thermal resistance, σ is the standard deviation of the measurements and ω_i is a random number chosen from a normal distribution with mean zero, variance one and standard deviation one.

4.1 First numerical experiment: the electrothermal method

The electrothermal method just providing the average temperatures of the heat sources, the number of components of the vector R_{int} can not be very high. So we search a 4-component vector whose distribution is shown on Figure 8a and we illustrate the influence of the heat source configuration. In this part, we assume exact measurement data, then σ is set equal to zero in eqn.(33).

4.1.1 Heat source configuration 1

First we examine the case of five long and parallel heat sources shown in Figure 9. The stopping criterion is not satisfied in this case. The exact and estimated components of the vector R_{int} are given in Figure 10. We learn from this figure that the computed values are not in agreement with the exact values. We deduce that this heat source configuration does not permit to reach a sufficient sensitivity for the estimation of R_{int} in the case of the electrothermal method.

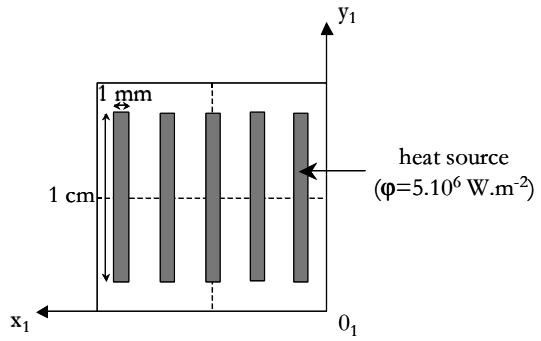

Figure 9. Heat source configuration 1 on the upper face of the element 1.

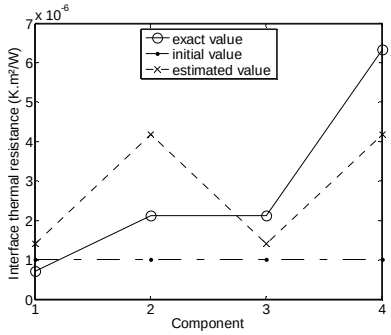

Figure 10. Estimation of the 4-component vector R_{int} (electrothermal method, heat source configuration 1, σ=0).

4.1.2 Heat source configuration 2

Now we choose to place one square heat source just in front of each zone of constant interface thermal resistance (see Figure 11). Figure 12 shows that this heat source configuration improves the sensitivity of the inverse method and leads to much more accurate results than the previous one. This estimation is obtained in only four iterations thanks to the gradient conjugate method.

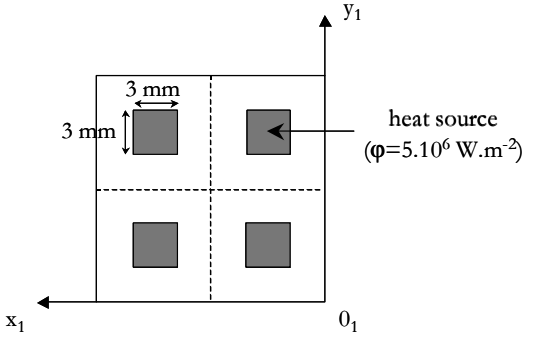

Figure 11. Heat source configuration 2 on the upper face of the element 1.

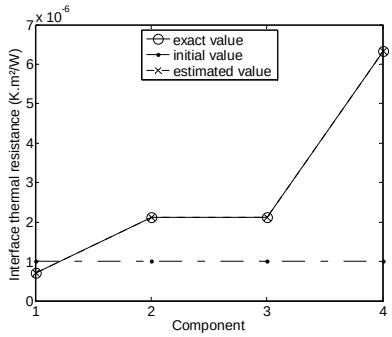

Figure 12. Estimation of the 4-component vector R_{int} (electrothermal method, heat source configuration 2, σ=0).

4.2 Second numerical experiment: the infrared thermography

Here we consider that an infrared camera provides a 20×20 temperature measurements grid. The grid locations are uniformly spaced on the upper face of the element 1. We are able to estimate a more discretized distribution than in part 4.1: a 16-component vector (Figure 8b) and a 64-component vector (Figure 8c). Besides, the measurement error for the infrared data is taken as σ is equal to 0.5K in eqn.(33), that is to say about 1% of the difference between the average and the minimum of the exact measured temperatures for the heat source configuration 1 and about 2% for the heat source configuration 2.

4.2.1 Estimation of a 16-component vector

Similar to the previous part, we compare the results obtained with the two heat source configurations. We note on Figure 13 that the two different configurations give a quite satisfactory distribution after 10 iterations. However, the minimization of the functional $J\left(\hat{R}_{\text{int}}^{k}\right)$ on Figure 14 shows that the configuration 2 requires less iterations than the configuration 1 to obtain an accurate estimation.

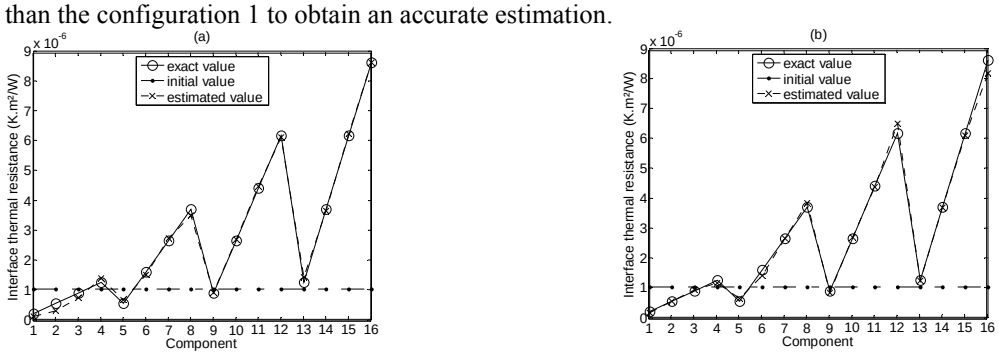

Figure 13. Estimation of the 16-component vector R_{int} after 10 iterations (infrared thermography, σ=0.5K): (a) heat source configuration 1, (b) heat source configuration 2.

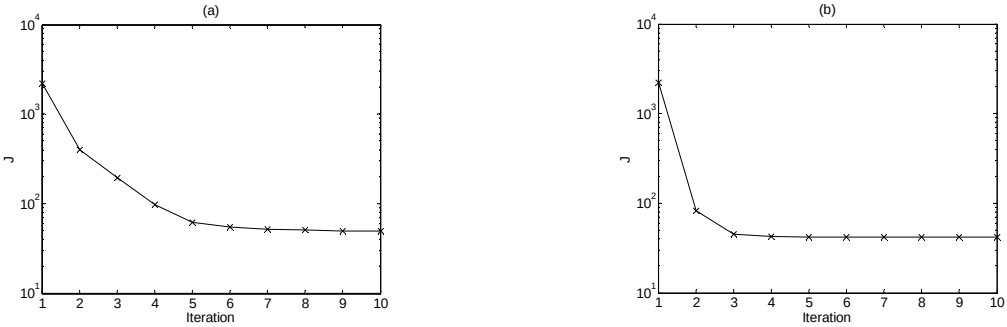

Figure 14. Evolution of the functional J for the estimation of the 16-component vector R_{int} (infrared thermography, σ=0.5K): (a) heat source configuration 1, (b) heat source configuration 2.

4.2.2 Estimation of a 64-component vector

To compute this estimation we use the heat source configuration 2 which seems to be more suitable for the identification of a high number of components. The evolution of the computed distributions for σ=0 (see Figure 15) shows that the estimation of a *nb*-component vector with no measurement error requires approximately *nb* iterations. We observe on Figure 16a the estimation obtained for σ=0.5K. Let us examine the covariance matrix related to the estimation of R_{int}. Its diagonal is composed by the squared standard deviations $\sigma^2_{\hat{R}^i_{int}}$ of the estimated components $\hat{R}^i_{int}$ (eqn.(34)) and allows us to estimate the relative error $\delta\hat{R}_{int}$ on the components of R_{int} (eqn.(35)):

$$cov(\hat{R}_{int}) = \sigma^2 (X^t X)^{-1} \text{ with } diag\left[cov(\hat{R}_{int})\right] = \left[\sigma^2_{\hat{R}^i_{int}}\right]_{i=1}^{i=nb} \tag{34}$$

$$\delta\hat{R}_{int} = \left[\frac{\sigma_{\hat{R}^i_{int}}}{R^i_{int}}\right]_{i=1}^{i=nb} \tag{35}$$

Figure 16b shows that we obtain a confident distribution ($\delta\hat{R}_{int} \leq 0.1$) on the zones where the gradient of the interface thermal resistance is the most important. On the contrary, the region where the gradient is poor (low x_1 and y_1 coordinates) leads to a less satisfactory estimation ($\delta\hat{R}_{int} \geq 0.5$).

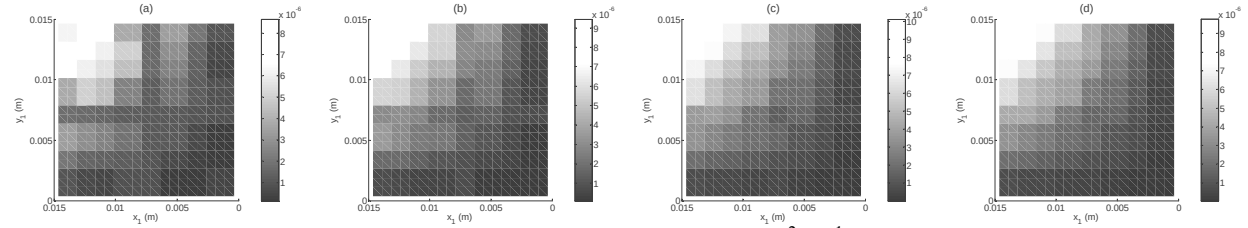

Figure 15. Estimated interface thermal resistance distributions ($K.m^2.W^{-1}$) for the 64-component vector R_{int} (infrared thermography, heat source configuration 2, σ=0): (a) 10 iterations, (b) 30 iterations, (c) 50 iterations, (d) 70 iterations.

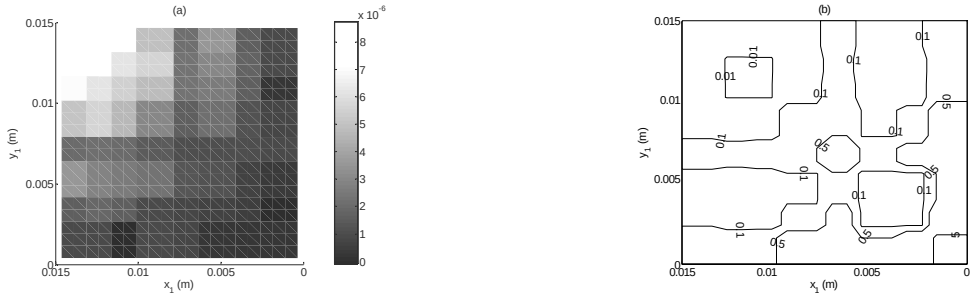

Figure 16. Estimation of the 64-component vector R_{int} (infrared thermography, heat source configuration 2, σ=0.5K): (a) estimated distribution $\hat{R}_{int}$ (K.m^2.W^{-1}), (b) isovalues of the relative error $\delta\hat{R}_{int}$.

We should note that this computation is quite heavy in terms of time calculation because the direct problem is solved *nb* times in the sensitivity problem at each iteration. This drawback could be avoided thanks to a function estimation approach using the conjugate gradient algorithm and the solution of the adjoint problem which constitutes the next step of this study.

5. CONCLUSIONS

The conjugate gradient method has been successfully applied for solving a 3-D steady-state inverse heat conduction problem to estimate the interface thermal resistance distribution of a die-attach material. A powerful thermal model has been developed for the direct problem. This model is particularly suitable to solve the 3-D heat conduction equation in microelectronics structures. The accuracy and the convergence rate of the inverse algorithm strongly depend on the heat source configuration chosen for the thermal excitation of the structure on the upper face of the semiconductor material. It appears that uniformly spaced square heat sources are more suitable than thin and parallel ones. Moreover, with no measurement error, the required number of iterations has to be equal at least to the number of unknowns of the discretized interface thermal resistance distribution. The influence of the measurements errors are also investigated and do not prevent to obtain a quite confident distribution. Finally, our calculation could be optimized by estimating both the values of the interface thermal resistance and the zonation, that is to say the partition of the interface whose parts correspond to the zones where the thermal resistance is constant, [1].

REFERENCES

1. H. B. Ameur, G. Chavent and J. Jaffré, Refinement and coarsening indicators for adaptive parametrization: application to the estimation of hydraulic transmissivities. *Inv. Prob.* (2002) **18**, 775-794.

2. A. Bendada, D. Maillet, J. C. Batsale and A. Degiovanni, Reconstitution of a non uniform interface thermal resistance by inverse conduction. *Inv. Prob. Eng.* (1998) **6**, 79-123.

3. V. Gatto, *Investigation of Thermal Phenomena in Power Electronic Components and Flexible Interconnect Systems for their Integration in an Automobile Engine Environment*, Ph.D. Thesis (Ecole Polytechnique de l'Université de Nantes), France, 2002, pp.81-105.

4. Y. Jarny, The adjoint method to compute the numerical solutions of inverse problems, *Inverse Engineering Handbook*, (ed. K. A. Woodbury), CRC Press, 2003, pp.103-217.

5. G. Maranzana, *Thermal Modeling of Power Electronics Components using the Thermal Quadrupoles*, Ph.D. Thesis (Institut National Polytechnique de Lorraine), France, 2003, pp.125-135.

6. G. Maranzana, I. Perry and D. Maillet, Quasi-analytical simulation of conduction heat transfer through a pyramidal multilayer multiblock. *Num. Heat Transfer, Part B* (2002) **42**, 499-521.

7. R. S. Pasher, C. Simmons and G. Solbrekken, Thermal contact resistance of phase change materials and grease type polymeric materials, *International Mechanical Engineering Congress and Exposition*, Orlando, Florida, 5-10 November, 2000, pp.461-466.

8. F. Raiszadeh and E. Derian, Thermal-mechanical measurements and analysis of an advanced thermal interface material construction, *17th IEEE Semi-Therm*, San Jose, California, 20-22 March, 2001, pp.63-70.